

# A Quick Review of an Electrodynamic Tether Experiment on the H-II Transfer Vehicle

IEPC-2017-359

*Presented at the 35th International Electric Propulsion Conference  
Georgia Institute of Technology • Atlanta, Georgia • USA  
October 8 – 12, 2017*

Yasushi Ohkawa<sup>1</sup>, Kentaro Iki<sup>2</sup>, Teppei Okumura<sup>3</sup> and Satomi Kawamoto<sup>4</sup>  
*Japan Aerospace Exploration Agency, Chofu, Tokyo, 182-8522, Japan*

*and*

Yuuta Horikawa<sup>5</sup>, Koichi Inoue<sup>6</sup>, Yuki Kobayashi<sup>7</sup>, Takashi Uchiyama<sup>8</sup> and Toru Kasai<sup>9</sup>  
*Japan Aerospace Exploration Agency, Tsukuba, Ibaraki, 305-8505, Japan*

**Abstract:** An electrodynamic tether (EDT) is a prospective candidate for the deorbit propulsion of active debris removal systems because it can contribute to simplifying the overall system and thus lowering the cost. In order to demonstrate some essential technologies for EDT, JAXA planned and conducted an on-orbit experiment of the EDT on the H-II transfer vehicle 6 (HTV-6). This plan is called KITE. The flight components of KITE have been installed to the HTV-6 until July 2016 and the freight was launched in December 2016. After the HTV left the international space station, the KITE mission began at the end of January 2017. Although tether deployment was unsuccessful due to malfunction, the field emission cathode and other mission components operated well and important on-orbit data were obtained.

## Nomenclature

$J_{et}$	=	emitter current of field emission cathode (electron current emitted from emitter material), mA
$J_{es}$	=	emission current of field emission cathode (electron current extracted from cathode unit), mA
$J_g$	=	gate current of field emission cathode (electron current through gate electrode), mA
$V_g$	=	gate voltage of field emission cathode, V
$\phi_H$	=	electrical potential of HTV with reference to plasma space potential, V

## I. Introduction

REMOVING large debris objects from crowded low Earth orbit (LEO) is one of the essential ways to prevent the ongoing growth of the space debris population. Some reports indicated that removing five large pieces of space debris from the crowded orbits per year will stop the continuous growth of the debris population.<sup>1,2</sup> In order to pursue

---

<sup>1</sup> Associate Senior Researcher, Research and Development Directorate, okawa.yasushi@jaxa.jp.

<sup>2</sup> Researcher, ditto.

<sup>3</sup> Researcher, ditto.

<sup>4</sup> Senior Researcher, ditto.

<sup>5</sup> Researcher, ditto.

<sup>6</sup> Unit Leader, Space Technology Directorate 1.

<sup>7</sup> Engineer, Human Spaceflight Technology Directorate.

<sup>8</sup> Flight Director, ditto.

<sup>9</sup> Senior Engineer, ditto.

ADR activities continuously, low-cost ADR systems should be developed. An electrodynamic tether (EDT)<sup>3</sup> is a prospective candidate for the deorbit propulsion of ADR systems because it can contribute to lowering the cost.

EDT is a propulsion system utilizing the ionosphere and planetary magnetic fields. Figure 1 shows a conceptual drawing of EDT and its application to ADR. Major advantages of EDT as the deorbit propulsion for ADR are as follows;

- 1) It requires no propellant because the thrust (electromagnetic force) is generated by electromagnetic interaction between the tether current and the geomagnetic field.
- 2) High electrical power is not necessary as self-induced electromotive force can drive the tether current.
- 3) No thrust vector control is required because the electromagnetic force is spontaneously generated against the orbital motion.
- 4) Restriction on clamping point and force on debris is not strict due to low and distributed thrust.

These advantages can contribute to simplifying the ADR systems and thus lowering the total cost. On the other hand, EDT has some disadvantages such as the potential possibility of tether cut by small debris or meteoroids during the operation, the impacts on other operational satellite due to the large effective cross-sectional area of the system, and no on-orbit demonstration performed as the deorbit propulsion device. We have to consider these disadvantages in developing EDTs for ADR.

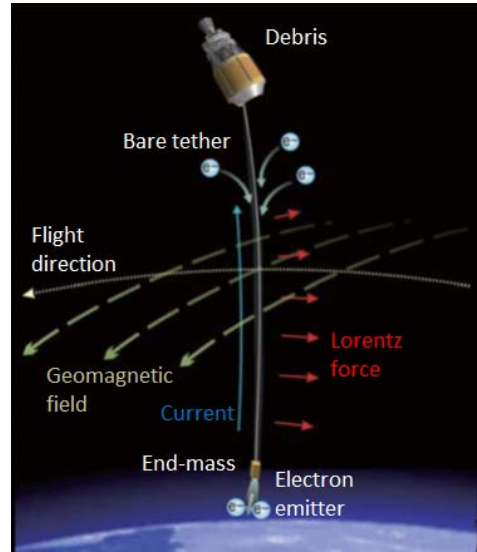
In order to demonstrate some essential technologies for EDT, JAXA planned an on-orbit EDT experiment on the H-II transfer vehicle 6 (HTV-6). This plan is called the Kounotori Integrated Tether Experiment (KITE). Figure 2 shows the expected image of KITE on orbit. EDT demonstration has been performed or planned many times<sup>4-9</sup> and many important data on the EDT fundamentals have been obtained in these experiments, however, our original experiment in space should be conducted to design and develop the EDT propulsion system for ADR.

## II. Overview of KITE mission

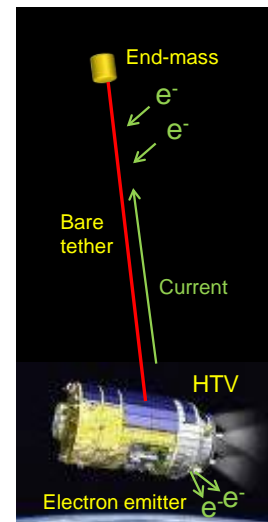
The primary objectives of KITE are to demonstrate the key EDT technologies such as a net-shaped bare tether possessing high tolerance to small-debris impact and a field emission cathode (FEC) as a small and simple electron source and to increase technology readiness levels to design and develop the EDT system for ADR. The 700-m-length bare tether collects electrons from the ambient space plasma, and the FEC on the HTV emits 10-mA-level electrons into the plasma. This combination of the plasma contactors can provide complete propellant-free deorbit propulsion. Table 1 shows the planned major mission specifications of KITE,

**Table 1. Major mission specifications of KITE (planned).**

Platform	H-II Transfer Vehicle 6 (HTV-6)
Mission duration	7 days
Orbit	20 km (or more) below ISS orbit (Altitude: 300 – 400 km, Inclination: 52 deg.)
Tether deployment direction	Zenith
Tether length	700 m (approx.)
Tether current	10 mA (approx.)
Electron collector	Bare tether
Electron emitter	Field emission cathode




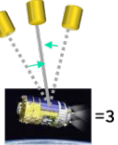


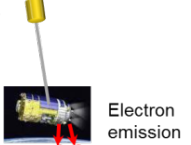
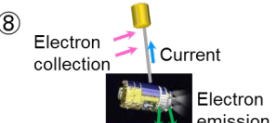
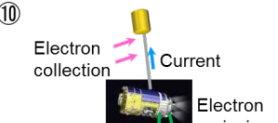
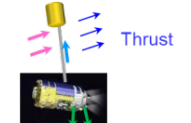
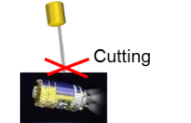
**Figure 1. Conceptual drawing of electrodynamic tether for active space debris removal.**



**Figure 2. Mission image of KITE.**

which were determined to achieve the mission objectives under some restrictions. Deorbiting of the HTV is beyond the scope because the expected EDT thrust is low.

The planned sequence of event of KITE is summarized in Fig. 3. Following events were planned in the 7-day mission. On Day 1, the tether is deployed after the checkout of KITE components and the tether vibration amplitude is alleviated using HTV thrusters. On Day 2, the tether vibration behavior, the tether voltage induced by the self-induced electromotive force, and the tether current due to the transfer of charged particles from/to the ambient plasma are measured. On Day 3, the initial characteristics measurement of the FEC is done, following the HTV potential measurement with and without electron emission. On Day 4, changes in the tether current and voltage are measured during the repetition of the on/off operation of the FEC. On Day 5, the FEC is operated in an autonomous mode and the autonomous operation of the EDT system is demonstrated. On Day 6, EDT thrust measurement is to be attempted by monitoring the tether vibration amplitude. On Day 7, the tether is severed to avoid causing troubles for the re-entry operation of the HTV.

Day	Event	Image
Day 1	①Checkout of KITE Components	 
	②End-mass Ejection (Tether Deployment)	
	③Tether Motion Alleviation by HTV Maneuver	
Day 2	④Observation of Tether Dynamics & ⑤Measurement of Electromotive Force	 
	⑥Checkout & Characteristics Measurement of Field Emission Cathode ⑦Measurement of HTV Electric Potential with and without Electron Emission	
Day 4	⑧Repetitive Measurement of Tether Electric Potential & Current	
Day 5	⑨Tether Motion Alleviation by HTV Maneuver (If required) ⑩Autonomous EDT Operation at Several Settings	
	⑪Autonomous EDT Operation at Maximum Electron Emission for EDT Thrust Measurement by Monitoring Tether Libration	
Day 7	⑫Extra Time for Additional Tests ⑬Cutting of Tether from HTV	

**Figure 3. Planned sequence of event in KITE.**

### III. KITE Components

The major components for KITE are the bare tether, reels for housing and braking, end-mass, releasing mechanism of the end-mass, camera for tether dynamics observation, FEC, electrical potential monitor (LP-POM), magnetic sensor (MAGS), and data handling unit/power control unit (DHU/PCU). Figure 4 shows the locations of the components on the HTV.

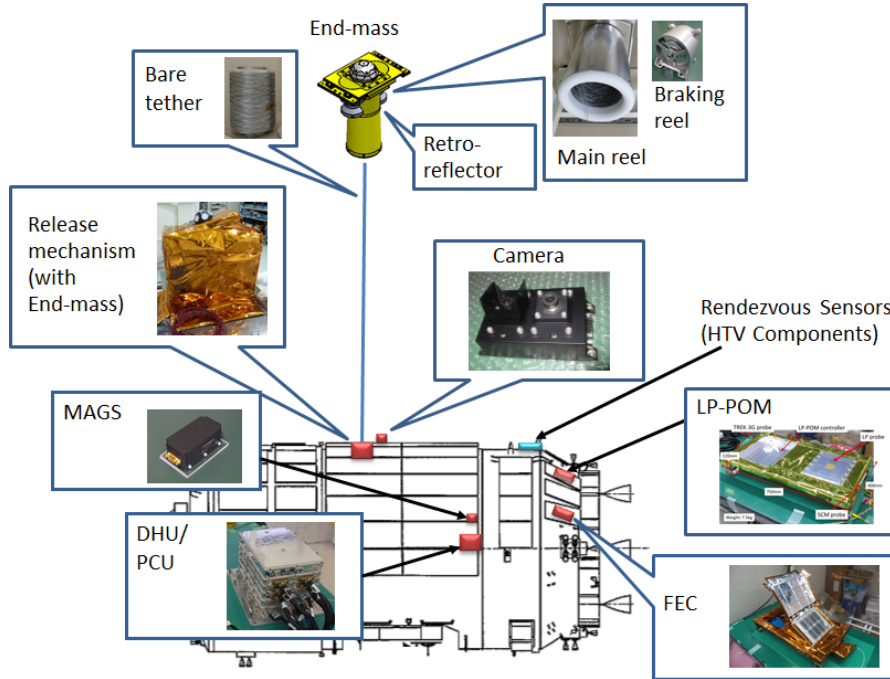


Figure 4. KITE components on HTV.

#### A. Tether and Reel <sup>10</sup>

The tether is housed in the end-mass in the initial condition. The total length of the tether is approximately 720 m. The tether has a mesh structure, as shown in Fig. 5, in order to avoid being cut by impacts from small-sized debris. Each yarn comprises a thin aluminum and stainless-steel wire. The surface of the initial 10 m of the tether at the HTV side is insulated by a non-conductive coating to avoid unintentional electrical discharge adjacent to the HTV body.

The last 10 m of the tether is connected to a drum-type braking reel. At the end of the deployment, the velocity of the end-mass is decelerated gradually by the braking reel and the deployment terminates gently without rebounding or severing.

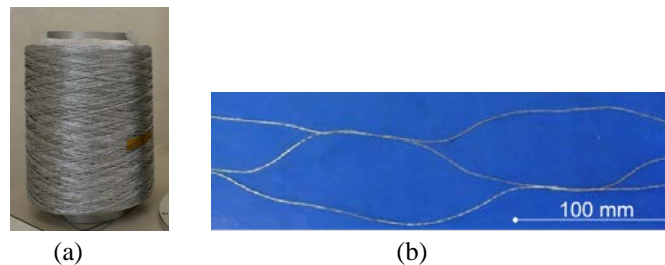


Figure 5. Bare tether. (a) 720-m-length tether rolled around core. (b) Close-up view of tether. (Gaps between yarns are widened intentionally.)

## B. Release Mechanism

The release mechanism comprises a spring for pushing out the end-mass and non-explosive actuators for holding the end-mass before its release. The action of the release is initiated by the execution of three individual commands for satisfying the safety requirement from the HTV. The initial velocity of the end-mass given by the release mechanism is designed to be approximately 1 m/s.

## C. Rendezvous Sensor (HTV Component)

The motion of the end-mass is observed and analyzed by rendezvous sensors (RVSs) of the HTV. The RVSs are not KITE components but original HTV instruments, which are used for approaching the International Space Station (ISS). The end-mass could be simplified using the RVSs because the position sensors, communication devices, and power sources were not required. Retroreflectors for the detection by the RVSs are mounted around the end-mass instead.

## D. Camera

A camera system is installed adjacent to the release mechanism in order to monitor the end-mass and tether. The system comprises two individual sets of lens and CMOS sensor; one of which is used for observing the motion of the end-mass just after the release so that the lens is telephoto, and the other is used for monitoring the tether motion so that the lens is wide-angled. The onboard processing logic, such as feature point recognition and image trimming, is implemented.

## E. Field Emission Cathode (FEC)

An FEC is used to emit electrons to the ambient space plasma. A schematic drawing of the FEC is shown in Fig. 6. Carbon nanotube (CNT) based FECs have been researched and developed in JAXA<sup>11</sup> and one of the laboratory models was improved and integrated for KITE.

An FEC module (see Fig. 7) is installed on the thruster module of the HTV as shown in Fig. 8. The FEC module comprises the FEC-Head (FECH), which emits electrons, the FEC-Controller (FECC), which provides high-voltage (HV) power to the FECH, the FEC-Guard (FECG), which covers the FECH until the mission starting. The FECG was opened just before the electron emission sequence started on Day3. The electron emission surface of the FECH is set parallel to the orbital direction to avoid having damage due to the direct impact of atomic oxygen flow.

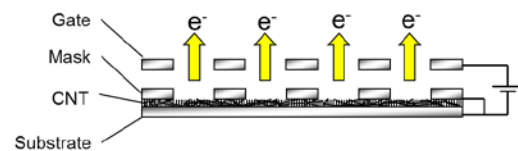


Figure 6. Schematic of FEC.

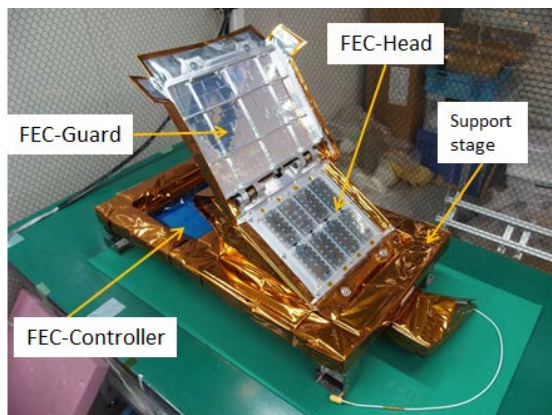


Figure 7. FEC module.

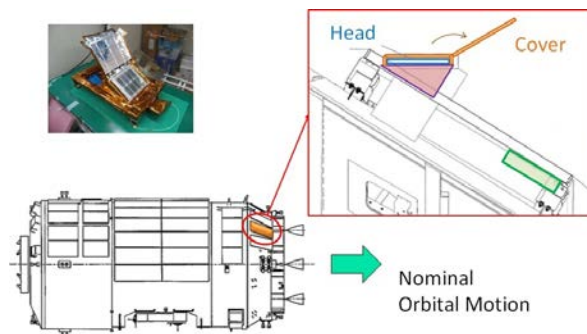


Figure 8. FEC module on HTV.

Figure 9 shows the FECH comprising eight cathode units (CUs). Each CU is operated using an independent HV DC converter in the FECC. A nominal electron emission capability of a single cathode unit is approximately 2.2 mA.

A simplified schematic of the electrical circuit including the FECH and FECC is shown in Fig. 10. The cable from the tether is connected to the emitter of the FECH through a switching unit containing three relays for avoiding discharge failure. This switching circuit was designed referring previous works.<sup>4,5</sup> A single HV converter drives one CU so that the gate voltage of each CU is independently controlled and the malfunction of a single HV or CU does not lead to a complete loss of function.

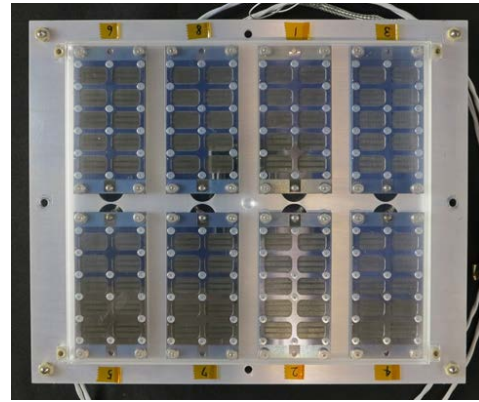


Figure 9. FECH.

#### F. Potential Monitor (LP-POM)

An electrical potential monitor with a plasma current probe (LP-POM) is installed on the thruster module of the HTV, as shown in Fig. 4. LP-POM measures the electrical potential of the HTV body with reference to the ambient space plasma. This function is indispensable for estimating the end-to-end tether voltage because this voltage is calculated as the summation of the absolute electrical potential of the HTV and the tether voltage measured at the switching unit in the FECC. Two kinds of potential sensors were installed and the function has been verified by the ATOTIE-mini experiment<sup>13</sup> on the HTV-4. Another function of the LP-POM is to measure the electron current from the ambient plasma using a planar probe. The number densities of the ambient plasma can be roughly estimated using this data. This function was demonstrated by the KASPER experiment on the HTV-5 in 2015.<sup>14</sup>

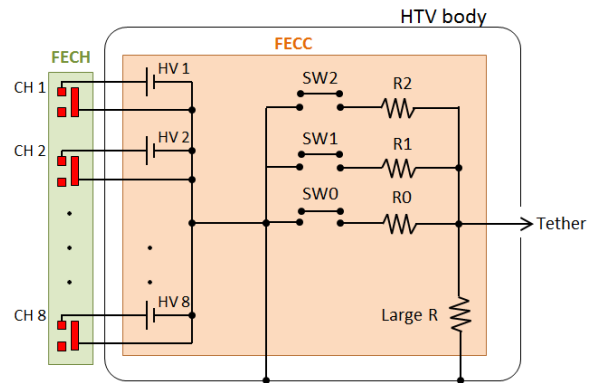


Figure 10. Schematic of EDT electrical circuit including FECC and FECH.

#### G. Magnetic Sensor (MAGS)

A MAGS is fixed inside of the main body of the HTV. MAGS measures the magnetic flux density of the geomagnetic field for supporting the analyses of the EDT characteristics. Although the data from the existing geomagnetic field model is probably enough to investigate the EDT characteristics, MAGS is effective to complement the data in case unexpected fluctuations of the geomagnetic field occur.

#### H. Data Handling Unit/Power Control Unit (DHU/PCU)

The data handling and power control of KITE components are ruled by a single device called DHU/PCU. DHU/PCU possesses the functions of data acquisition for KITE components, telemetry/command interpretation between the HTV and KITE, and electrical power distribution to KITE components. DHU/PCU is installed next to the MAGS in the HTV main body.

## IV. Quick Review of KITE Results

#### A. Results Overview

The flight components of KITE have been installed to the HTV-6 until July 2016 and the freight was launched in December 2016. The HTV-6 left the ISS after the successful transportation operation, and the KITE mission was conducted from January 28 to February 5, 2017.

Table 2 summarizes the daily events in the KITE mission. On Day 1, following the initial checkout of the KITE instruments, the end-mass ejection process for tether deployment was pursued, however, release of the end-mass was not detected. On Day 2, investigation on the malfunction and plans for retrieval were discussed. After Day 2, both the re-attempts to deploy the tether and the operation of FEC were conducted in parallel or serial. Despite various efforts and attempts to recover the malfunction, the end mass could not be released at the end. The KITE mission was terminated just before HTV-6 began re-entry maneuver.

Although the tether deployment was unsuccessful, the FEC operated well without any critical trouble throughout the mission period. Some additional tests on FEC, such as the electron emission operation at various HTV attitude, which was not planned in original, were conducted using an extra mission time.

Other KITE components were also functioning well without fatal problems. LP-POM was continuously operated from the HTV launch to the re-entry. The electrical potential of the HTV body and the plasma current were obtained at the all HTV operation phases; solo-flight, docking to the ISS, berthing at the ISS, releasing from the ISS, and the KITE mission. MAGS also worked well during the KITE mission acquiring three-axis magnetic flux density. The camera could not be used for monitoring the end-mass and tether, however, images of the ISS, which are effective for developing visual guidance and navigation systems for ADR, were acquired during the rendezvous phase.<sup>15</sup> DHU/PCU performed its roll perfectly.

In the following section, results of FEC operation were described in detail.

## B. Results of FEC Operation

The FEC operation was started on Day 3 by opening the FECG and ended on Day 8 by obtaining the final I-V characteristics. All eight cathode units operated throughout the mission period without any critical failure, such as a short-circuit between the electrodes. Table 3 shows the summary of FEC operation results. The accumulated operation time reached 50 hours in the total exposure time of 130 hours. The total maximum emitter current and emission current were approximately 10 and 6 mA, respectively. “Emitter current” indicates the electron current emitted from the CNT emitter and “emission current” means the electron current extracted to outside the cathode units. The emission current is calculated by subtracting the gate current from the emitter current.

### 1. Electron emission to plasma without tether

The first point to be discussed on the FEC operation in KITE is whether the electrons were really emitted to the ambient plasma in this experiment, in which a bare tether did not exist. In the EDT fundamentals, the tether generates

**Table 2. Overview of daily events in KITE.**

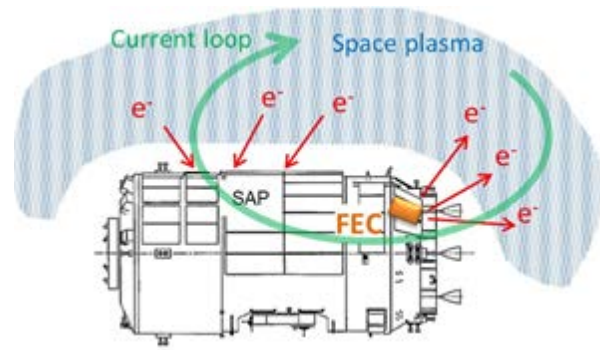
Day	Event
Day 1	Checkout of KITE components.
	Tether deployment attempt. Resulted in unsuccessful.
Day 2	Discussion on tether deployment malfunction.
Day 3	Opening of FECG.
	Measurement of I-V characteristics of FEC.
Day 4	Successive FEC operation at low current level.
Day 5	Tether deployment re-attempt. Unsuccessful.
	Measurement of I-V characteristics of FEC.
Day 6	Tether deployment re-attempt. Unsuccessful.
	Successive FEC operation at high current level.
Day 7	Successive FEC operation at three different current levels.
	Successive FEC operation at three different HTV Yaw attitude .
Day 8	Measurement of I-V characteristics of FEC.
	Shutdown of KITE components.

**Table 3. Summary of FEC operation.**

Accumulated operation time	50 h
Accumulated exposure time	130 h
Number of I-V measurement operation	84
Number of autonomous consecutive operation	22
Maximum emitter current (sum of 8 cathode units)	10.2 mA
Maximum emission current (sum of 8 cathode units)	5.8 mA

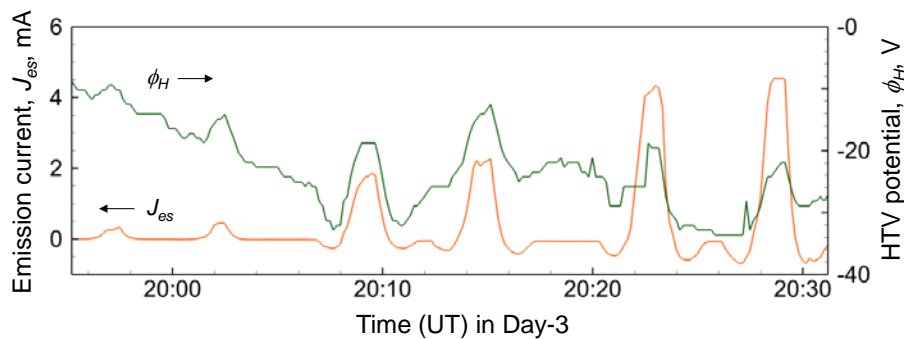
the potential difference between the tether ends, and thus the electron current loop via the electron emitter, ambient plasma and bare tether is formed in a steady state.

We infer that the voltage generated by the HTV's solar cells plays a role of the tether voltage, and the exposed anodic potential area of the solar cells collects electrons from the ambient plasma. Figure 11 illustrates the conceptual image of the current loop formation via space plasma in this experiment.



**Figure 11. Electrical current loop via ambient space plasma by electron emission from FEC and collection at solar cells.**

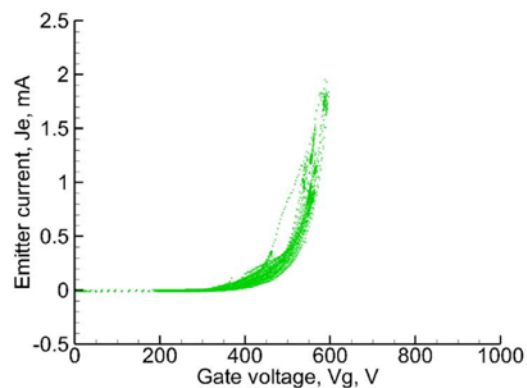
Figure 12 shows supporting evidence of the inference above. This figure shows the trends in electrical potential of the HTV and in emission current from the FEC at the initial current-voltage characteristics measurement on Day 3. The potential and current were obtained by LP-POM and FECC, respectively. There is a correlation between the HTV potential and emission current, that is, the negative potential of the HTV was mitigated by the electron emission from the FEC. This relation indicates that the potential balance between the HTV and the space plasma in the nominal condition was violated by the electron emission from FEC, thus establishing a new potential equilibrium. These data also indicate that FEC can be applied to control or mitigate spacecraft charging for preventing malfunction caused by unintended discharges.



**Figure 12. Trends in electrical potential of HTV and electron emission current from FEC.**

### 2. Current-voltage characteristics of FEC on-orbit

An example of current-voltage (I-V) characteristics of a single cathode unit is shown in Fig. 13. This figure shows the relationship between the emitter current and gate voltage of the No. 4 cathode unit obtained at the initial I-V measurement on Day 3. Measurement results at several times of voltage-sweep are plotted here. Typical characteristics in field emission phenomena were observed from this figure.



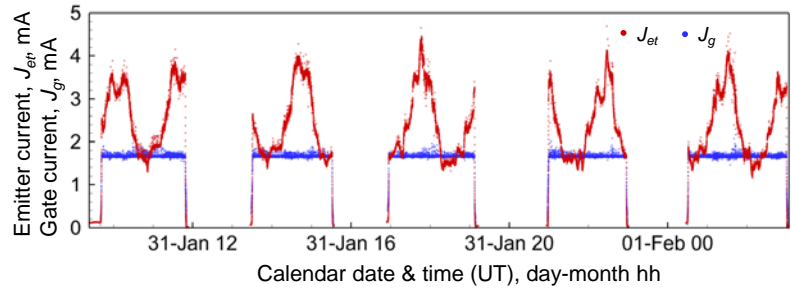
**Figure 13. Typical example of current-voltage characteristics of single cathode unit. Data was obtained on Day 3 for No. 4 cathode unit.**

### 3. Trend in electron emission in accordance with HTV potential variation

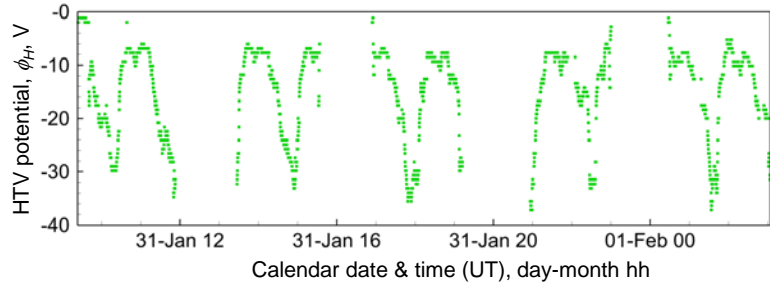
Figure 14 shows an example of the trend in total emitter and gate current when the eight cathode units operated simultaneously. Results of five successive autonomous operations on Day 4 were shown in this



figure. The electrical potential of the HTV with reference to ambient plasma at the same time range is also shown in the figure. The intermissions between the operations are attributable to recording and downlinking of the data. The gate current was kept almost constant and the emitter current widely varied in magnitude. These results show that the gate voltage of each cathode unit was adjusted to maintain constant gate current as intended, and the emitter current varied depending on the HTV potential. The trend in HTV potential largely depends on the voltage generation by the HTV's solar cells, that is, the solar irradiation conditions. The emitter current is larger when the HTV potential is lower. This tendency is reasonable because the space charge limit is mitigated when the potential difference between the FEC and the plasma becomes larger.



(a) Emitter and gate current.



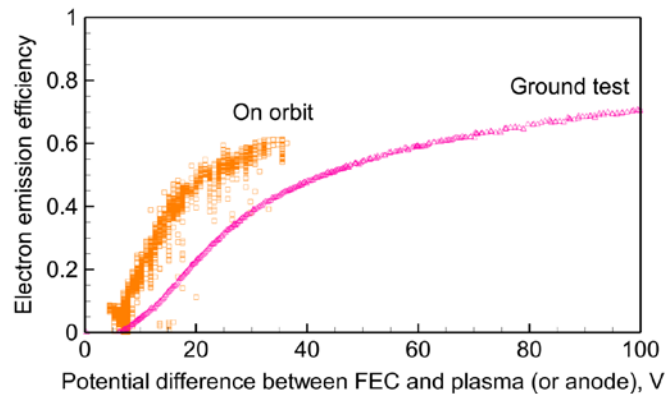
(b) Electrical potential of HTV with reference to ambient plasma.

#### 4. Electron emission efficiency

One of the essential indicators to characterize the FEC performance is the electron emission efficiency against the anode (or plasma on-orbit) potential. Note that “electron emission efficiency” indicates the ratio of emission current to emitter current. This indicator is important for estimating the tether current in the EDT system under various potential conditions. Figure 15 shows the electron emission efficiency plotted against the plasma-to-HTV potential difference during the autonomous operation on Day 6. The results at the final ground test of the FECH are also shown in this figure. The plate anode located 200 mm away from FECH was used for current collection in the ground test.

The on-orbit data in Fig. 15 shows that emission efficiency depends on the plasma-to-HTV potential difference as expected, and that the characteristics are better than those obtained by the ground test using the plate anode.

**Figure 14. Trend in electron emission characteristics and HTV potential on Day 4. Data in five successive autonomous operations are plotted.**



**Figure 15. Electron emission efficiency plotted against plasma-to-HTV potential difference. Result of ground test is also plotted as reference.**

## V. Conclusion

The mission concept, components, and results of the electrodynamic tether experiment on the H-II transfer vehicle were reviewed. Although the tether could not be deployed due to the malfunction of the end-mass release mechanism, the field emission cathode and other mission components operated well throughout the mission period. Obtained on-orbit data on the field emission cathode are effective to understand the electron emission phenomena in the ionosphere and to develop the cathode devices for future active debris removal systems.

## Acknowledgments

The authors wish to thank the KITE team and the HTV team for their significant efforts and supports in pursuing the project. This work was partly supported by JSPS KAKENHI Grant Number JP16H04595.

## References

- <sup>1</sup> Liou, J-C, "An update on the effectiveness of post mission disposal in LEO," *Inter-Agency Space Debris Coordination Committee*, IAC-13-A6.4.2, Beijing, China, September 2013.
- <sup>2</sup> Liou, J-C., "An Update on LEO Environment Remediation with Active Debris Removal," *Orbital Debris Quarterly News*, Vol. 15, Issue 2, April 2011, pp. 4-6.
- <sup>3</sup> Drell, S. D., Foley, H. M., and Ruderman, M. A., "Drag and Propulsion of Large Satellites in the Ionosphere: An Alfvén Propulsion Engine in Space," *Journal of Geophysical Research*, Vol. 70, No. 13, pp. 3131-3145, 1965.
- <sup>4</sup> Stone, N. H., "Electrodynamic characteristics of the Tethered Satellite System during the TSS-1R mission," *Space Programs and Technology Conference*, Huntsville, September 1996, AIAA-96-4472.
- <sup>5</sup> Vaughn, J. A., Curtis, L., et al., "Review of the ProSEDS electrodynamic tether mission development," *40th Joint Propulsion Conference*, Fort Lauderdale, July 2004, AIAA-2004-3501.
- <sup>6</sup> Lilley, J. R., Greb, A. Jr., et al., "Comparison of Theoretical Calculations with Plasma Motor Generator (PMG) Experimental Data," *32<sup>nd</sup> Aerospace Sciences Meeting*, Reno, January 1994, AIAA-1994-0328.
- <sup>7</sup> Sasaki, S., Oyama, K. I., et al., "Results from a Series of Tethered Rocket Experiments," *Journal of Spacecraft and Rockets*, Vol. 24, No. 5, 1987, pp. 444-453.
- <sup>8</sup> Watanabe, T, Fujii, H. A., et al., "T-Rex: Bare Electro-Dynamic Tape-Tether Technology Experiment on Sounding Rocket S520," *Journal of Space Technology and Science*, Vol. 26, No. 1, 2012, pp. 14-20.
- <sup>9</sup> Nohmi, M., "Initial Orbital Performance Result of Nano-Satellite STARS-II," *12<sup>th</sup> International Symposium on Artificial Intelligence, Robotics and Automation in Space*, Montreal, June 2014.
- <sup>10</sup> Iki, K, Kawamoto, S., et al., "The Expected On-orbit Tether Deployment Dynamics on KITE Mission," *30<sup>th</sup> International Symposium on Space Technology and Science*, ISTS-2015-r-27, Kobe, Japan, July 2015.
- <sup>11</sup> Ohkawa, Y., Matsumoto, K., Kawamoto, S., and Kitamura, S., "Performance Improvement of a Carbon Nanotube Field Emission Cathode," *63rd International Astronautical Congress*, IAC-12-C4.4.11, Naples, Italy, October 2012.
- <sup>12</sup> Shimada, A., Tanaka, Y., et al., "Effect of Atomic Oxygen Irradiation on Field Emission Cathodes in Low Earth Orbit," *Trans. JSASS Aerospace Tech. Japan*, Vol. 12, No. ists29, pp. Pb\_59-Pb\_64, 2014.
- <sup>13</sup> Okumura, T., Tsujita, D., et al., "On-orbit Potential Measurement of H-II Transfer Vehicle," *13th Spacecraft Charging Technology Conference*, Pasadena, June 2014.
- <sup>14</sup> Okumura, T., Kawakita, S., et al., "On-orbit Potential Measurement of H-II Transfer Vehicle-5," *14<sup>th</sup> Spacecraft Charging Technology Conference*, Netherlands, April 2016.
- <sup>15</sup> Kimura, S., Horikawa, Y., and Katayama, Y., "Quick Report on On-Board Demonstration Experiment for Autonomous-Visual-Guidance Camera System for Space Debris Removal," *31st International Symposium on Space Technology and Science*, ISTS-2017-r-40, Matsuyama, Japan, June 2017.